

# The Optimal Design of Standard Gears\*

Michael Savage,† John J. Coy,‡ and Dennis P. Townsend§

The design of a gearset is a reasonably difficult problem which involves the satisfaction of many design constraints. In recent literature, several approaches to the optimum design of a gear mesh have been presented (refs. 1 to 3). Cockerham (ref. 1) presents a computer design program for 20° pressure angle gearing which ignores gear-tooth tip scoring. This program varies the diametral pitch, face width, and gear ratio to obtain an acceptable design. Tucker (ref. 2) and Estrin (ref. 3) look more closely at the gear-mesh parameters, such as addendum ratio and pressure angle, and outline procedures for varying a standard gear mesh to obtain a more favorable gearset. Gay (ref. 4) considers gear tip scoring as well and shows how to modify a standard gearset to bring this mode of failure into balance with the pitting fatigue mode. He also adjusts the addendum ratios of the gear and pinion to obtain an optimal design.

No general procedures exist, however, to determine the optimal size of a standard gear mesh. The basic approach available is one of checking a given design to verify its acceptability (refs. 5 to 7).

Optimum methods are presented for the design of a gearbox (refs. 8 to 10) with the object of minimizing size and weight. These methods focus on multistage gear reductions and consider the effect of splitting the gear ratios on overall transmission size.

The optimum design of a standard gearset has not been treated in the literature to date. Such a study must be based on a thorough study of the kinematics of the gear mesh, such as those by Buckingham (ref. 11) and Anderson (ref. 12). The gear strengths that must be considered include bending fatigue as treated by the AGMA (ref. 13), by Gitchel (ref. 14), and by Mitchiner and Mabie (ref. 15). Surface pitting of the gear teeth in the full load region must also be treated (refs. 16 to 18) as must gear scoring at the tip of the gear tooth (refs. 19 and 20).

The objective of the research reported here is to establish an optimal design procedure for spur gear pairs. Standard tooth forms are assumed. Figure 1 shows a single mesh of the external type, and figure 2 shows a single mesh of the internal type. The procedure developed in this paper uses standard gear geometry and optimizes the remaining parameters to obtain the most compact standard gearset for a given application of specified speed reduction and input torque. The procedure applies to internal and external gearing.

## Nomenclature

<i>a</i>	addendum ratio
<i>C</i>	center distance, m
<i>d</i>	dedendum ratio
<i>E</i>	elastic modulus, Pa
<i>F</i>	tangential tooth load, N
<i>f</i>	gear face width, m
<i>k</i>	slope of equal size design line in design space
<i>l</i>	parabolic beam height, m
<i>m<sub>g</sub></i>	gear ratio
<i>m<sub>p</sub></i>	contact ratio
<i>N</i>	tooth number

\*Work partially supported by NASA Grant NAG3-55.

†The University of Akron.

‡Propulsion Laboratory, U.S. Army Research and Technology Laboratories (AVRADCOM), NASA Lewis Research Center.

§NASA Lewis Research Center.

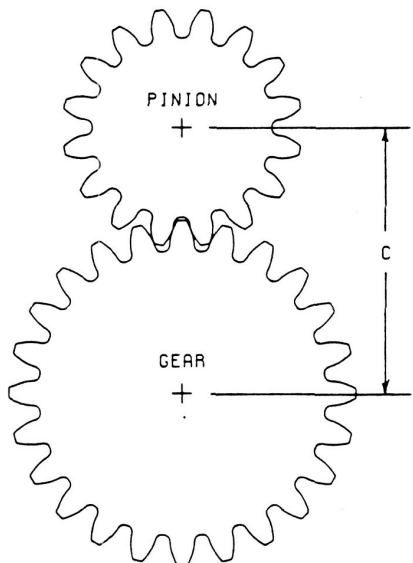


Figure 1. - External gear mesh.

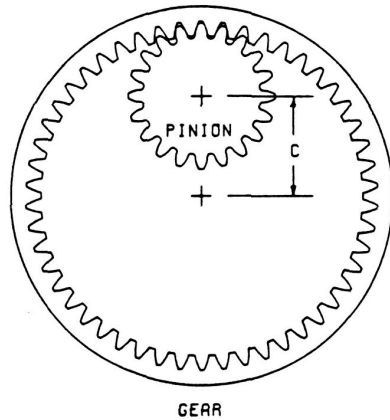


Figure 2. - Internal gear mesh.

$n$	number of million stress cycles
$P_d$	diametral pitch
$p_b$	base pitch, m
$R$	pitch radius, m
$R_a$	addendum radius, m
$R_b$	base circular radius, m
$S$	probability of survival
$T_p$	pinion torque, N·m
$t$	parabolic beam depth, m
$V$	stress volume, m <sup>3</sup>
$Y$	Lewis tooth form factor
$Z$	length of action, m
$z_o$	depth to maximum shearing stress, m
$\beta$	secondary interference angle, deg
$\gamma$	secondary interference gear rotation angle, deg
$\delta$	roll angle to initial point of contact, deg
$\theta$	involute correction angle, deg
$\theta_B$	pinion roll angle to lowest point of single tooth contact, rad
$\theta_c$	pinion roll angle to lowest point of tooth contact, rad
$\lambda$	length to diameter ratio
$\nu$	Poisson's ratio
$\rho$	radius of curvature, m
$\sigma_B$	bending fatigue stress, Pa
$\sigma_{BT}$	bending fatigue stress for load at the pinion tooth tip, Pa
$\sigma_N$	surface pressure, Pa
$\sigma_{NT}$	surface pressure at the gear tooth tip, Pa
$\tau$	shearing stress, Pa

TABLE 1 GEAR MESH PARAMETER CONSTRAINTS

Parameter	Description	Equality constraint
$N_1$	Pinion tooth number	
$m_g$	Gear ratio	$m_g = (m_g)_{\text{design}}$
$N_2$	Gear tooth number	$N_2 = m_g N_1$
$P_d$	Diametral pitch	
$R_1$	Pinion pitch radius	$R_1 = N_1/2P_d$
$R_2$	Gear pitch radius	$R_2 = N_2/2P_d$
$C$	Center distance	$C = R_2 + R_1$
$a_1$	Pinion addendum ratio	1 for std tooth form
$a_2$	Gear addendum ratio	1 for std tooth form
$d_1$	Pinion dedendum ratio	1.25 for std tooth form
$d_2$	Gear dedendum ratio	1.25 for std tooth form
$f$	Mesh face width	$f = \lambda N_1/P_d$
$\phi$	Pitch line pressure angle	$\phi = \phi_{\text{STD}}$
$E_1$	Pinion radius	
$v_1$	Pinion Poisson's ratio	Pinion
$\sigma_{B1}$	Pinion bending design stress	Material properties
$\sigma_{N1}$	Pinion surface design pressure	
$E_2$	Gear modulus	
$v_2$	Gear Poisson's ratio	Gear
$\sigma_{B2}$	Gear bending design stress	Material properties
$\sigma_{N2}$	Gear surface design pressure	

Table 1 includes four parameter groups, addendum and dedendum ratios, face width, pressure angle, and material constants, which are tied down by standard practice but which could be varied in the design of nonstandard gearing. Several other parameters are determined exactly in terms of the input specifications and the free parameters. One parameter is a design input quantity, and only two parameters are free to be varied over an arbitrary range of values. These two free parameters in this formulation of the gear-mesh design problem are the number of teeth on the pinion and the diametral pitch. This leaves the designer with a two-dimensional design space for standard gears and a six-dimensional design space for nonstandard gears.

The design spaces are limited by the inequality constraints of the problem. These inequality constraints could generate a null design space by placing conflicting requirements on the free parameters. In a well posed design problem, they will enclose a bounded area of acceptable designs.

To assure a quiet mesh, the contact ratio of the mesh should be greater than some minimum value. The value 1.4 is commonly stated (refs. 6 and 7), but higher values will make the mesh even quieter. For reasonable manufacturing of the gear teeth, both the tooth tip and the tool tip should be wider than a specified minimum (ref. 3). These widths permit proper surface hardening of the tooth and prevent excessive tool tip wear in manufacture. For standard gearing, these three inequalities are automatically satisfied by the standard.

For proper tooth engagement and disengagement, involute interference (contact below the base circle) and secondary interference between the pinion tooth tip and the internal gear tooth tip for internal gearing must be avoided.

For proper gear mesh strength and life, the possibility of failure by three different mechanisms must be avoided. These mechanisms are pinion-tooth bending fatigue, surface fatigue, or spalling in the region of single-tooth load and gear-tip scoring.

To treat these three modes of failure on a common basis, a nominal stress approach is used. A three modes of failure are affected by more than the nominal design stress used herein. The bending fatigue is dependent on the surface finish of the tooth among other factors (refs. 6 and 7). The surface fatigue of the tooth is influenced by the stress volume and does not have an infinite endurance limit (ref. 17). The gear tip scoring failure is highly temperature dependent (ref. 2).

TABLE 1 GEAR MESH PARAMETER CONSTRAINTS

Parameter	Description	Equality constraint
$N_1$	Pinion tooth number	
$m_g$	Gear ratio	$m_g = (m_g)_{\text{design}}$
$N_2$	Gear tooth number	$N_2 = m_g N_1$
$P_d$	Diametral pitch	
$R_1$	Pinion pitch radius	$R_1 = N_1/2P_d$
$R_2$	Gear pitch radius	$R_2 = N_2/2P_d$
$C$	Center distance	$C = R_2 + R_1$
$a_1$	Pinion addendum ratio	1 for std tooth form
$a_2$	Gear addendum ratio	1 for std tooth form
$d_1$	Pinion dedendum ratio	1.25 for std tooth form
$d_2$	Gear dedendum ratio	1.25 for std tooth form
$f$	Mesh face width	$f = \lambda N_1/P_d$
$\phi$	Pitch line pressure angle	$\phi = \phi_{\text{STD}}$
$E_1$	Pinion radius	
$v_1$	Pinion Poisson's ratio	Pinion
$\sigma_{B1}$	Pinion bending design stress	Material properties
$\sigma_{N1}$	Pinion surface design pressure	
$E_2$	Gear modulus	
$v_2$	Gear Poisson's ratio	Gear
$\sigma_{B2}$	Gear bending design stress	Material properties
$\sigma_{N2}$	Gear surface design pressure	

Table 1 includes four parameter groups, addendum and dedendum ratios, face width, pressure angle, and material constants, which are tied down by standard practice but which could be varied in the design of nonstandard gearing. Several other parameters are determined exactly in terms of the input specifications and the free parameters. One parameter is a design input quantity, and only two parameters are free to be varied over an arbitrary range of values. These two free parameters in this formulation of the gear-mesh design problem are the number of teeth on the pinion and the diametral pitch. This leaves the designer with a two-dimensional design space for standard gears and a six-dimensional design space for nonstandard gears.

The design spaces are limited by the inequality constraints of the problem. These inequality constraints could generate a null design space by placing conflicting requirements on the free parameters. In a well posed design problem, they will enclose a bounded area of acceptable designs.

To assure a quiet mesh, the contact ratio of the mesh should be greater than some minimum value. The value 1.4 is commonly stated (refs. 6 and 7), but higher values will make the mesh even quieter. For reasonable manufacturing of the gear teeth, both the tooth tip and the tool tip should be wider than a specified minimum (ref. 3). These widths permit proper surface hardening of the tooth and prevent excessive tool tip wear in manufacture. For standard gearing, these three inequalities are automatically satisfied by the standard.

For proper tooth engagement and disengagement, involute interference (contact below the base circle) and secondary interference between the pinion tooth tip and the internal gear tooth tip for internal gearing must be avoided.

For proper gear mesh strength and life, the possibility of failure by three different mechanisms must be avoided. These mechanisms are pinion-tooth bending fatigue, surface fatigue, or spalling in the region of single-tooth load and gear-tip scoring.

To treat these three modes of failure on a common basis, a nominal stress approach is used. All three modes of failure are affected by more than the nominal design stress used herein. The bending fatigue is dependent on the surface finish of the tooth among other factors (refs. 6 and 7). The surface fatigue of the tooth is influenced by the stress volume and does not have an infinite life endurance limit (ref. 17). The gear tip scoring failure is highly temperature dependent (ref. 22).

However, this temperature is a direct result of the contact pressure and sliding velocity at the gear tip. The contact pressure is thus a meaningful parameter to predict the severity of both surface pitting and tip scoring. The nominal tooth bending stress will also be used as a measure of the bending fatigue severity.

Once all these limits have been applied to the design space, the designer is in a position to survey the acceptable designs and select the optimum. The criterion of this selection, called the merit function, is established as the center distance of the gears. By minimizing the center distance at a specified load, one produces the most economical gearset for the stated conditions since it would use the least material for the gears and permit the gearbox to assume a minimum size. This criterion could be inverted very easily if a fixed size was available for the gearset. The merit function would then become the maximum transmitted load for the given size or the maximum reliability for a given size and load.

## Kinematic Interference

Involute interference occurs when the addendum circle of one gear crosses the line of action past the point of tangency with the base circle on the mating gear. For standard tooth systems with equal addenda, the pinion will always be the gear on which contact occurs below the base circle. The contact geometry is shown in figure 3 for an external gear and in figure 4 for an internal gear. Involute interference occurs when the gear tooth contacts the pinion tooth below its involute profile. The relation that describes this is a comparison of two distances. For contact with an external gear (fig. 3) the distance between the points of tangency of the line of action with the two base circles,  $A$  and  $E$ , should be greater than the distance on the gear along this line of action from the addendum circle,  $B$ , to the point of tangency with its base circle,  $E$ ;

$$AE > BE \quad (1)$$

or

$$C \sin \varphi > \sqrt{R_{a2}^2 - R_{b2}^2} \quad (2)$$

for no primary interference.

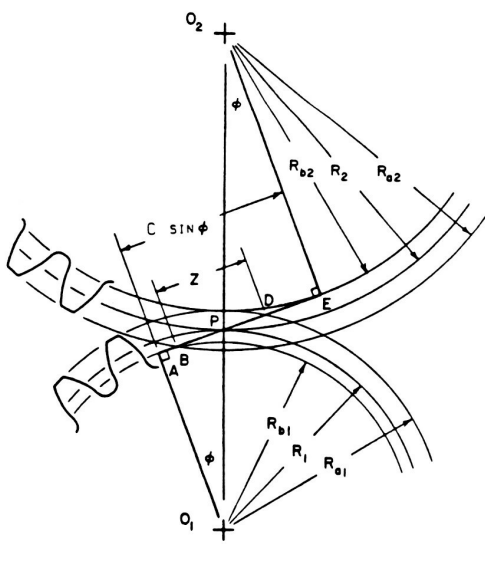


Figure 3. - Pinion - external gear mesh geometry.

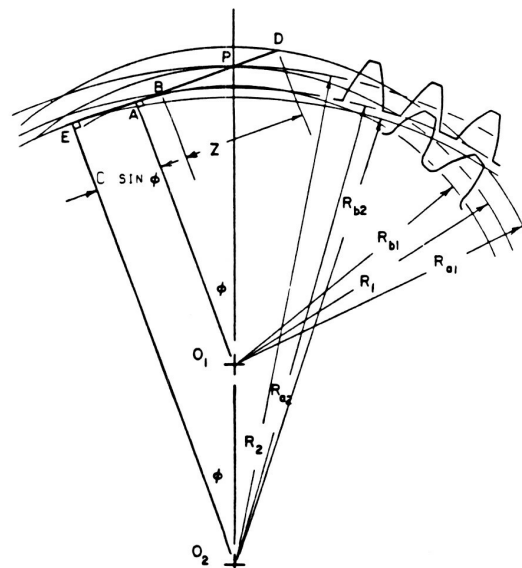


Figure 4. - Pinion - internal gear mesh geometry.

The standard cure for primary involute interference is to increase the number of teeth on the pinion for the desired gear ratio until the inequality is satisfied. These relationships can be used to define a minimum number of teeth required to avoid interference. Since

$$C = R_1 + R_2 \quad (3)$$

$$R_1 = \frac{N_1}{2P_d} \quad (4)$$

$$R_2 = \frac{N_2}{2P_d} \quad (5)$$

$$R_{b2} = R_2 \cos \varphi = \frac{N_2 \cos \varphi}{2P_d}, \quad (6)$$

and

$$R_{a2} = R_2 + \frac{a_2}{P_d} = \frac{N_2}{2P_d} + \frac{a_2}{P_d} \quad (7)$$

one has

$$\left( \frac{N_1 + N_2}{2P_d} \right) \sin \varphi > \sqrt{\left( \frac{N_2}{2P_d} + \frac{a_2}{P_d} \right)^2 - \left( \frac{N_2}{2P_d} \cos \varphi \right)^2} \quad (8)$$

multiplying through by  $2P_d/N_2$ , and solving for  $N_2$  yields

$$N_2 > \frac{2a_2}{\sqrt{\cos^2 \varphi + \left( \frac{1}{m_g} + 1 \right)^2 \sin^2 \varphi - 1}} \quad (9)$$

or, in terms of  $N_1$ ,

$$N_1 > \frac{2a_2/m_g}{\sqrt{\cos^2 \varphi + \left( \frac{1}{m_g} + 1 \right)^2 \sin^2 \varphi - 1}} \quad (10)$$

for contact with an external gear.

For contact with an internal gear (fig. 4) the distance between the points of tangency of the line of action with the two base circles,  $\overline{EA}$ , should be less than the distance on the gear along the line of action from the addendum circle,  $B$ , to the point of tangency with its base circle,  $E$ .

$$\overline{EA} < \overline{EB} \quad (11)$$

$$C \sin \varphi < \sqrt{R_{a2}^2 - R_{b2}^2} \quad (12)$$

In this case

$$C = R_2 - R_1 \quad (13)$$

and

$$R_{a2} = \frac{N_2}{2P_d} - \frac{a_2}{P_d} \quad (14)$$

Thus,

$$\left(\frac{N_2 - N_1}{2P_d}\right) \sin \varphi < \sqrt{\left(\frac{N_2}{2P_d} - \frac{a_2}{P_d}\right)^2 - \left(\frac{N_2}{2P_d}\right) \cos^2 \varphi} \quad (15)$$

Multiplying through by  $2P_d/N_2$  and solving for  $N_2$  yields

$$N_2 > \frac{2a_2}{1 - \sqrt{\cos^2 \varphi + \left(1 - \frac{1}{m_g}\right)^2 \sin^2 \varphi}} \quad (16)$$

or, in terms of  $N_1$ ,

$$N_1 > \frac{2a_2/m_g}{1 - \sqrt{\cos^2 \varphi + \left(1 - \frac{1}{m_g}\right)^2 \sin^2 \varphi}} \quad (17)$$

for contact with an internal gear.

By satisfying relation 10 or 17, one can assure that primary involute interference will not occur for a given gear ratio, pressure angle, and gear addendum ratio. This check is sufficient for all cases in which the gear addendum ratio equals the pinion addendum ratio, as is the case for standard gears.

However, if the pinion addendum ratio were greater than that on the gear, one would also have to check interference on the gear tooth. For contact with an external gear, the pinion addendum must cross the line of action inside the point of tangency between the line of action and the gear base circle.

$$AD < AE \quad (18)$$

The resulting limit on the number of pinion teeth is

$$N_1 > \frac{2a_1}{\sqrt{\cos^2 \varphi + (1 + m_g)^2 \sin^2 \varphi} - 1} \quad (19)$$

for contact with an external gear.

To avoid interference with the base of the internal gear tooth, the addendum radius of the gear must be greater than its base radius.

$$R_{a2} > R_{b2} \quad (20)$$

$$\frac{N_2}{2P_d} - \frac{a_2}{P_d} > \frac{N_2}{2P_d} \cos \varphi \quad (21)$$

or

$$N_2 > \frac{2a_2}{1 - \cos \varphi} \quad (22)$$

In terms of  $N_1$  this becomes

$$N_1 > \frac{2a_2/m_g}{1 - \cos \varphi} \quad (23)$$

For standard teeth with  $a_2 = 1.0$ , this requires  $N_2$  to be greater than 34 teeth for a  $20^\circ$  pressure angle or 22 teeth for a  $25^\circ$  pressure angle. This does not pose a problem for standard teeth.

For contact with an internal gear a second type of kinematic interference is possible in which the tip of the internal gear contacts the tip of the pinion as they come into mesh (refs. 11 and 12). This interference, called "fouling," is illustrated in figure 5. In this figure two mating gears are shown in contact at the pitch point,  $P$ . The clearance between the teeth can be seen three or four teeth away from the pitch point. However, as one moves further from the pitch point to the intersection of the two addendum circles, interference between the tips of teeth on the two gears can be seen.

To avoid this secondary interference, or fouling, the actual rotation of the gear tooth caused by the rotation of the pinion tooth must be greater than the rotation of the gear tooth that would allow interference. The actual rotation of the pinion tooth is given by

$$\gamma_1 = \beta_1 + \theta_1 \quad (24)$$

Where  $\beta_1$  is the angle from the pitch point to the intersection of the addendum circles on the pinion. It can be found from the law of cosines that

$$\beta_1 = \cos^{-1} \left( \frac{R_{a2}^2 - R_{a1}^2 - C^2}{2CR_{a1}} \right) \quad (25)$$

The angle  $\theta_1$  is the angle on the pinion tooth between the pitch circle and the addendum circle. It is given by

$$\theta_1 = \text{inv } \varphi_{a1} - \text{inv } \varphi \quad (26)$$

where  $\varphi$  is the pitch line pressure angle and  $\varphi_{a1}$  is the pressure angle at the addendum circle. The involute function (ref. 7) is shown in figure 6 and is related to the involute curve's pressure angle by

$$\text{inv } \varphi = \tan \varphi - \varphi \quad (27)$$

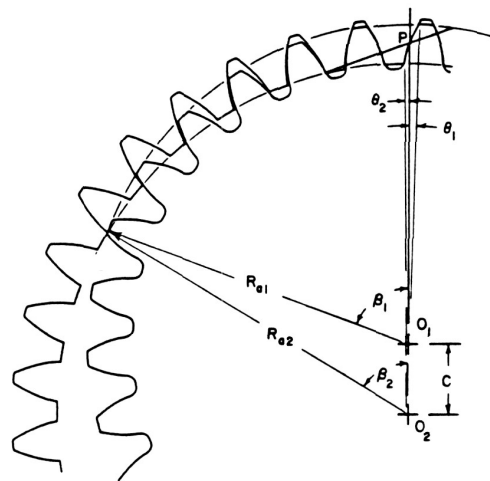


Figure 5. - Secondary interference geometry.

where  $\varphi$  is measured in radians for this calculation.

The rotation limit of the gear is given by

$$\gamma_2 = \beta_2 - \theta_2 \quad (28)$$

where  $\beta_2$  is the angle from the pitch point to the intersection of the addendum circles on the gear, found from  $\beta_1$  by the law of sines, such that

$$\beta_2 = \sin^{-1} \left( \frac{R_{a1} \sin \beta_1}{R_{a2}} \right) \quad (29)$$

and where  $\theta_2$  is the angle on the gear tooth between the pitch circle and the addendum circle, that is,

$$\theta_2 = \text{inv } \varphi - \text{inv } \varphi_{a2} \quad (30)$$

Since the actual gear rotation must be greater than this rotation limit for a rotation of  $\gamma_1$  of the pinion,

$$\frac{\gamma_1}{m_g} > \gamma_2 \quad (31)$$

to avoid secondary interference or fouling.

## Contact Ratio

The contact ratio for a given spur gear mesh is the ratio of the length of action along the line of action between the two addendum circles to the base pitch:

$$m_p = \frac{Z}{p_b} \quad (32)$$

In this equation

$$p_b = \frac{\pi}{P_d} \cos \varphi \quad (33)$$

where the base pitch,  $p_b$ , is defined as the distance from one tooth to the next, measured along the line of action. The length of contact,  $Z$ , can be expressed as

$$Z = \overline{BD} = \sqrt{R_{a1}^2 - R_{b1}^2} + \sqrt{R_{a2}^2 - R_{b2}^2} - C \sin \varphi \quad (34)$$

for contact with an external gear as shown in figure 3. Combining these equations yields

$$m_p = \frac{N_1}{2\pi \cos \varphi} \left[ \sqrt{\left(1 + \frac{2a_1}{N_1}\right)^2 - \cos^2 \varphi} + \sqrt{\left(m_g + \frac{2a_2}{N_1}\right)^2 - m_g^2 \cos^2 \varphi} - (1 + m_g) \sin \varphi \right] \quad (35)$$

For contact with an internal gear (fig. 4) the length of contact,  $Z$ , is given by

$$Z = \sqrt{R_{a1}^2 - R_{b1}^2} - \sqrt{R_{a2}^2 - R_{b2}^2} + C \sin \varphi \quad (36)$$

The contact ratio for this case can be expressed as

$$m_p = \frac{N_1}{2\pi \cos \varphi} \left[ \sqrt{\left(1 + \frac{2a_1}{N_1}\right)^2 - \cos^2 \varphi} - \sqrt{\left(m_g - \frac{2a_2}{N_1}\right)^2 - m_g^2 \cos^2 \varphi} - (1 - m_g) \sin \varphi \right] \quad (37)$$

This contact ratio should be greater than 1.4 and is normally less than 2.0 for standard spur gears. For contact with an internal gear at low ratios and for nonstandard addenda and dedenda, it can exceed 2.0. For the strength modeling of this design study, it will be assumed to be less than 2.0.

## Gear-Tooth Strengths

Spur-gear teeth have three distinct modes of failure. A tooth may fail in bending fatigue at its root, it may fail by pitting fatigue on its surface, or it may fail by scoring at the tip of the gear tooth.

The basic model for bending failure of a gear tooth was developed by Wilfred Lewis in 1893 (ref. 15). Although the knowledge of fatigue strengths and this mechanism of failure have increased significantly since then, compensating factors exist that make the Lewis model of bending failure reasonably accurate. As a result, it is still the bending strength analysis in use today. The idea is to fit the largest possible constant-width, constant-surface-stress cantilever inside the tooth. The apex of this parabolic beam is placed at the intersection of the applied load and the centerline of the tooth (shown as point *b* in fig. 7). The strength of the tooth is then equated to the strength of this beam:

$$\sigma_L = \frac{Mc}{I} = \frac{6Fl}{f t^2} \quad (38)$$

where *F* is the tangential load in newtons, *l* is the parabola length in meters, *f* is the gear face width in meters, and *t* is the parabola depth at the critical tooth section in meters. Lewis has written this expression as

$$\sigma_L = \frac{FP_d}{fY} \quad (39)$$

where *Y* is the dimensionless Lewis form factor, which is a function of the proportion of the tooth and not its size.

$$Y = \frac{t^2 P_d}{6l} \quad (40)$$

The form factor *Y* can thus be determined by locating the point of tangency between the tooth fillet and the parabola inscribed within the tooth with its apex at *b* (labeled *a* in fig. 7).

The length, *t*, is the full thickness of the parabola at this point, while *l* is the distance between points *b* and *a* along the tooth centerline. These distances can be found by an iterative scheme which finds the point of the fillet for which the tangent to the fillet crossed the centerline of the tooth at *c*, a distance *l* above the parabola apex—point *b*. This tangent will also be tangent to the inscribed parabola with its apex at *b*. This calculation (refs. 14 and 15) requires knowledge of the tip radius of the tool, the addendum and dedendum of the gear tooth as well as the pitch line pressure angle of the tooth. These four quantities are fixed for a given standard gear system. The procedure assumes that the tooth width and tooth space are equal at the pitch radius.

In addition, the iteration procedure requires knowledge of the number of teeth on the gear and the pressure angle at the point on the involute surface of the tooth at which the load is acting. This pressure angle increases from zero at the base radius to the nominal pressure angle at the pitch circle to a maximum pressure angle at the largest involute radius on the tooth. Standard tables (refs. 6 and 7) of tooth form factors give the factor for the load at the tooth tip or at the middle of the tooth for a given tooth system. The factors are then tabulated versus the number of teeth on the pinion since the

factor magnitude is independent of the physical size of the gear. The factor for the load at the tooth tip is given since this is for the largest effective cantilever loading on the tooth. However, at this point the load is shared with another mesh so a second point of concern is the highest point of single tooth load. This point is approximated by placing the load at the middle of the tooth for tabular purposes. A more correct procedure is to use the highest point of single tooth contact. This point varies with the gear ratio and can be found from an analysis of the mesh geometry. Once found, it is defined by the pressure angle,  $\varphi_A$ , of the involute at that point. This pressure angle is related to the roll angle,  $\theta_A$ , of the involute as shown in figure 6. Here  $\theta_A$  is the angle of unwrap of the line of action from the base circle:

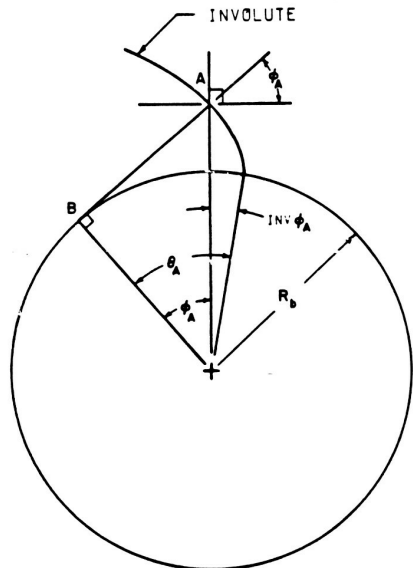


Figure 6. - Involute angle geometry.

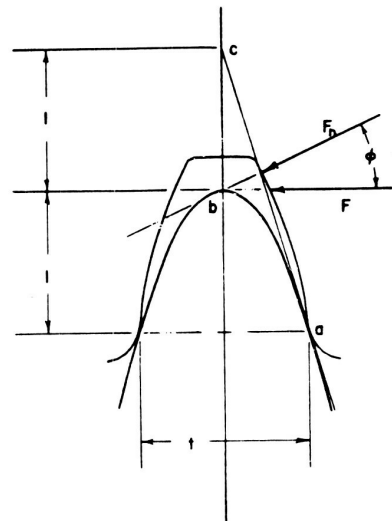


Figure 7. - Tooth bending strength model.

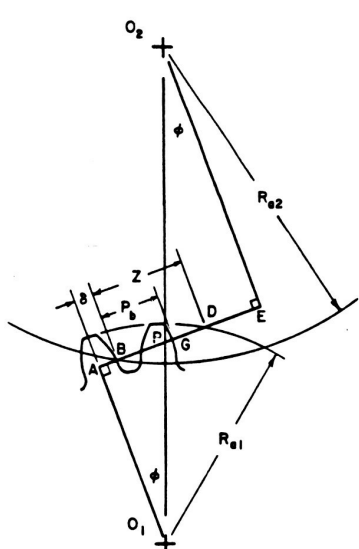


Figure 8. - Highest point of single tooth contact for an external gear mesh.

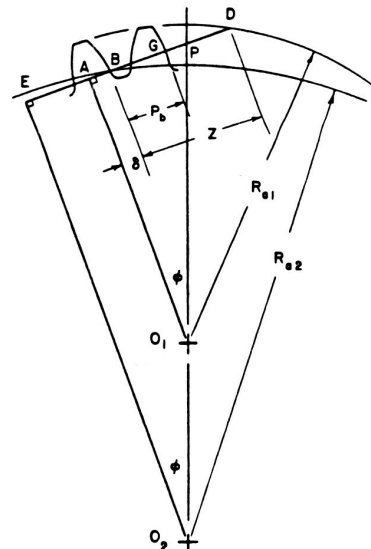


Figure 9. - Highest point of single tooth contact for an internal gear mesh.

$$\theta_A = \frac{\overline{AB}}{R_b} = \tan \varphi_A \quad (41)$$

hence,

$$\varphi_A = \tan^{-1} \theta_A \quad (42)$$

The roll angle to the highest point of single tooth contact can be determined by considering figure 8 for contact with an external gear and figure 9 for contact with an internal gear. In both cases the distance  $\overline{AD}$  is given by

$$\overline{AD} = \sqrt{R_{a1}^2 - R_{b1}^2} \quad (43)$$

and the distance  $\overline{GD}$  is given by

$$\overline{GD} = Z - p_b \quad (44)$$

The highest point of single tooth contact is at  $G$  and its roll angle is

$$\theta_A = \frac{AG}{R_{b1}} = \frac{\sqrt{R_{a1}^2 - R_{b1}^2} - (Z - p_b)}{R_{b1}} \quad (45)$$

Similarly, the roll angle to the lowest point of single tooth contact can be found by rolling the pinion until  $G$  corresponds to  $D$ . In this position the second tooth which was at  $B$  will have moved up to the start of single tooth contact. Thus,

$$\theta_B = \frac{\overline{AD} - p_b}{R_{b1}} \quad (46)$$

defines the roll angle to the lowest point of single tooth contact on the pinion tooth. It is at this point where the Hertzian pressure due to single tooth contact is a maximum.

It has been shown that the surface endurance of gear teeth behaves much like that of rolling-element bearings (ref. 17). The life of the contact is represented by

$$\ln \frac{1}{S} \sim \frac{\tau^c V n^e}{z_o^h} \quad (47)$$

where  $S$  is the probability of survival,  $\tau$  is the critical shear stress,  $n$  is the number of million stress cycles,  $z_o$  is the depth to the critical stress,  $e$  is the Weibull exponent, and  $c$  and  $h$  are material constants. The three design parameters in this expression are the stress, its depth, and the volume of material subjected to the stress. Since the depth of the critical shear stress is nearly fixed and since the stress is raised to a power in excess of three, relative to the volume, it is assumed in this study that the magnitude of surface compression is a reasonable measure of the tendency of the surface to pit. It is thus used as a criterion for design comparison.

The Hertzian pressure which produces spalling can be modeled by

$$\sigma_N = \sqrt{\frac{F}{\pi f \cos \varphi} \left( \frac{1/\rho_1 + 1/\rho_2}{\frac{1-\nu_1^2}{E_1} + \frac{1-\nu_2^2}{E_2}} \right)} \quad (48)$$

where  $\rho_1$  and  $\rho_2$  are the radii of curvature at the point of contact. For this study it will be assumed that the two gears are made of the same material. It can be seen from figures 10 and 11 that the

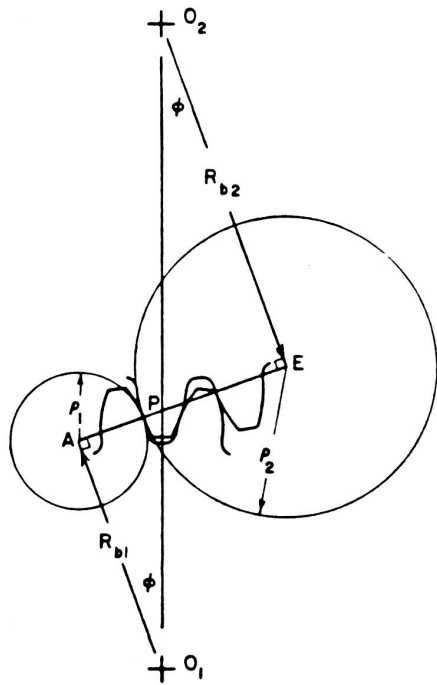


Figure 10. - Tooth surface curvature for an external gear mesh.

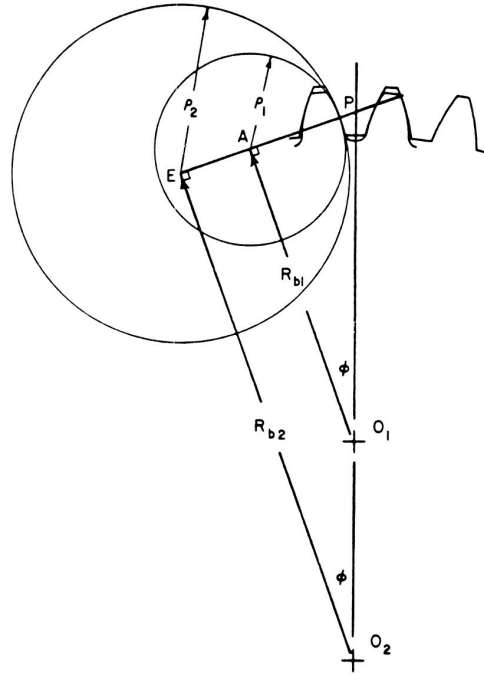


Figure 11. - Tooth surface curvature for an internal gear mesh.

centers of curvature of the two gear teeth surfaces are the points of tangency of the line of action with the respective base circles. Since these points are fixed, one has

$$\rho_2 = C \sin \varphi - \rho_1 \quad (49)$$

for the external gear and

$$\rho_2 = -C \sin \varphi - \rho_1 \quad (50)$$

for the internal gear where the minus sign indicates conformal contact. At the point of maximum Hertzian pressure, in the single-tooth contact region,

$$\rho_1 = \theta_B R_{b1} \quad (51)$$

Putting all this together, one has

$$\sigma_N = \sqrt{\frac{FE(C \sin \varphi)}{2(1-\nu^2)\pi f \cos \varphi (\theta_B R_{b1})(C \sin \varphi \mp \theta_B R_{b1})}} \quad (52)$$

where the minus sign holds for contact with an external gear and the plus sign holds for contact with an internal gear.

The scoring mode of failure is more difficult to predict since it is influenced by a combination of factors. Scoring is caused by an instability in oil film thickness at high speed and high load with inadequate cooling. In addition to surface pressure, this mode of failure is affected by the relatively large sliding velocity present at the gear tip and by the temperature of the teeth. Because of the sliding velocity present, some elastohydrodynamic effects are present in the contact that alter the pressure distribution from the simple Hertzian model of equation (48). Oil cooling has a major effect in preventing scoring.

A second factor exists which increases the tip pressure above that of the simple model. That factor is dynamic loading, which is largest at the initial point of contact. When the pinion drives the gear making the mesh a speed reduction, this point of initial contact is the gear tooth tip and the base of the pinion tooth. Because of the complexities involved in dynamic load estimation, the contact pressure at the gear tip is modeled by equation (48). In this case the radius of curvature on the pinion tooth is given by

$$\rho_1 = \overline{AB} = \sqrt{R_{a1}^2 - R_{b2}^2} - Z \quad (53)$$

and the radius of curvature of the gear tooth is given by equation (49) for an external gear or equation (50) for an internal gear. The roll angle to this point of contact on the pinion is

$$\theta_c = \frac{\overline{AB}}{R_{b1}} \quad (54)$$

and

$$\sigma_{NT} = \sqrt{\frac{FE(C \sin \varphi)}{2(1 - \nu^2)\pi f \cos \varphi(\theta_c R_{b1})(C \sin \varphi \mp \theta_c R_{b1})}} \quad (55)$$

gives the surface pressure.

Although contact pressure is only one factor in this mode of failure, it is a significant one. If this pressure is extreme, the design is not in balance, and excessive measures must be taken in the other factors to compensate. It is felt then that the contact pressure at the gear tip should be kept to the same level as that in the single-tooth load region.

## Design Space

As shown in table I and described in the section on parameters and constraints, the standard gear design problem for gears made of a chosen material can be reduced to a two-dimensional design problem where the two free parameters are the number of teeth on the pinion and the diametral pitch.

The inequality constraints which bound this design space are the minimum number of teeth required to prevent interference and the three strength limits. These strength limits can be converted to expressions for the maximum allowable diametral pitch for the given problem as functions of the number of teeth on the pinion. As stated in table I the face width can be expressed in terms of the length-to-diameter ratio of the gear tooth contact:

$$f = \lambda \frac{N_1}{P_d} \quad (56)$$

The load can also be expressed in terms of the diametral pitch:

$$F = \frac{T_p}{R_1} = \frac{2T_p P_d}{N_1} \quad (57)$$

For the bending limit where  $Y$  is taken as the tooth-form factor for the highest point of single-tooth contact for the given ratio and the number of teeth on the pinion, combining equations (39), (56), and (57) yields

$$\sigma_L = \frac{2T_p P_d^3}{Y \lambda N_1^2} \quad (58)$$

or in terms of the allowable bending strength  $\sigma_B$

$$P_d \leq \sqrt[3]{\frac{\sigma_B Y \lambda N_1^2}{2T_p}} \quad (59)$$

For the single-tooth pitting limit, equations (56) and (57) are combined with equation (52):

$$\sigma_N^2 = \frac{2T_p E P_d^3 \sin \varphi}{(1 - \nu^2) \pi \lambda N_1^2 \cos^2 \varphi (\theta_B N_1)} \left[ \sin \varphi \mp \frac{\theta_B \cos \varphi}{(m_g \pm 1.0)} \right] \quad (60)$$

where  $\theta_B$  is given by equation (46) and is a function of  $N_1$  and  $\varphi$ . This equation can also be solved for an upper bound on  $P_d$  as a function of  $N_1$  and the allowable surface wear pressure,  $\sigma_N$ :

$$P_d \leq \sqrt[3]{\frac{(1 - \nu^2) \pi \lambda N_1^3 \sigma_N^2 \cos^2 \varphi \theta_B}{2T_p E \sin \varphi}} \left[ \sin \varphi \mp \frac{\theta_B \cos \varphi}{(1 \pm m_g)} \right] \quad (61)$$

where the positive sign holds for contact with an external gear while the negative  $m_g$  is for contact with an internal gear.

Finally, a similar equation can be found for the limit on  $P_d$  based on gear-tooth tip scoring in terms of  $\theta_c$ , the roll angle on the pinion to the initiation of contact. This angle, as given by equation (54), is also a function of only  $N_1$  and  $\varphi$  for the stated problem:

$$P_d \leq \sqrt[3]{\frac{(1 - \nu^2) \pi \lambda N_1^3 \sigma_N^2 \cos^2 \varphi \theta_c}{2T_p E \sin \varphi}} \left[ \sin \varphi - \frac{\theta_c \cos \varphi}{(1 \pm m_g)} \right] \quad (62)$$

These limits are plotted in figure 12 for the case  $\varphi = 20^\circ$ ,  $m_g = 1.0$ ,  $\lambda = 0.25$ ,  $T_p = 113 \text{ N}\cdot\text{m}$  (1000 lb-in),  $E = 205 \text{ GPa}$  ( $30 \times 10^6 \text{ psi}$ ),  $\nu = 0.25$ ,  $\sigma_N = 1.38 \text{ GPa}$  (200 000 psi) and  $\sigma_B = 414 \text{ MPa}$  (60 000 psi). The gear for this design problem is external. The acceptable design space is the upper left hand corner of the plot.

The merit function for this problem is the center distance,  $C$ :

$$C = \frac{N_1}{2P_d} (m_g \pm 1) \quad (63)$$

where the plus sign is valid for an external gear, and the negative sign holds for an internal gear in equations (62) to (64). For a given gear ratio the locus of equally optimum designs can be found by considering  $C$  to be constant. This produces the relation

$$N_1 = \left[ \frac{2C}{(m_g \pm 1)} \right] P_d \quad (64)$$

which states that equally sized designs lie on a straight line through the origin. Since the smaller  $C$ , the better the design, the best design corresponds to the line of least slope drawn through the origin which lies within the design space. For this design the line of least slope within the design space crosses the two surface pressure limits at their intersection, point A in figure 12.

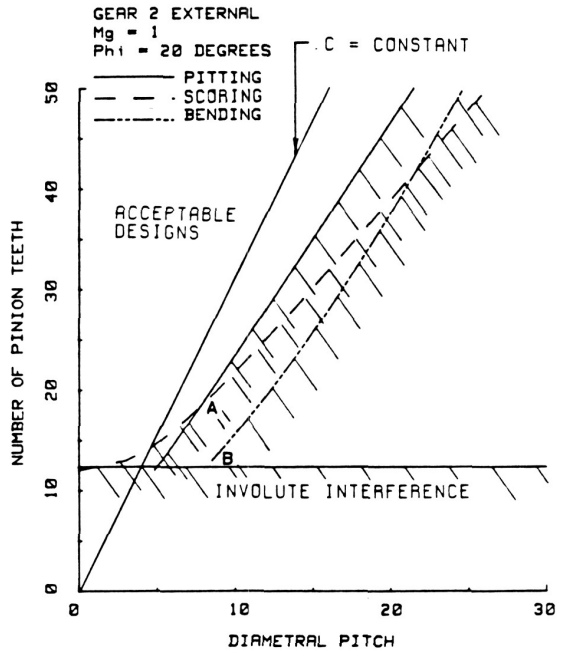


Figure 12

## Optimal Designs

In this study arbitrarily chosen values are used for the tooth width to pinion pitch diameter ratio,  $\lambda$ , and the pinion torque,  $T_p$ . Values of 0.25 and 113 N·m (1000 lb·in) were chosen to reflect reasonable geometry and a nominal load. The design spaces do not change in character as these quantities are varied, so no loss in generality results from their use. The values of elastic modulus, Poisson's ratio, allowed surface pressure and bending fatigue strength are for hardened steel. If another material is used for the gears, the design space would be altered. However, the only real difference would be a shift in the relative importance of the surface wear strengths and the bending strengths.

For high-speed, high-cycle operations, point *A* in figure 12 is an important design point since it identifies the minimum number of pinion teeth required to keep the gear-tooth tip contact pressure at or below the maximum contact pressure in the full-load region of the tooth surface. By having at least this number of teeth in the pinion, a well balanced compact design can be achieved by sizing the gears based on the full-load contact surface pressure.

It is of interest to note that this limit is close to a straight line through the origin. Exceeding this minimum number of teeth does not significantly change the merit function,  $C$ , if one stays on the constraint line for pitting. This is partly due to the fact that the radius of curvature of the teeth is more a function of the base circle size than the tooth size once one gets away from the situation of tooth contact near the base circle.

A common design approach (ref. 7) in the design of gearsets has been to use the interference limit and the tooth bending strength limit to define the "best" design. This gives point *B* in the design space of figure 12. This point will produce a smaller gearset, since  $OB$  has a smaller slope than  $OA$ , but it ignores the pitting problems in the full load region and totally ignores the situation at the tip of the gear tooth. It thus will produce gears that are not balanced in their design and that may have pitting and scoring problems in service.

The design space of figure 12 can be used to study the effects of varying the parameters  $N_1$  and  $P_d$  on a design with a gear ratio of 1 and a pressure angle of 20°. Similar design spaces can be drawn for different gear ratios and different pressure angles.

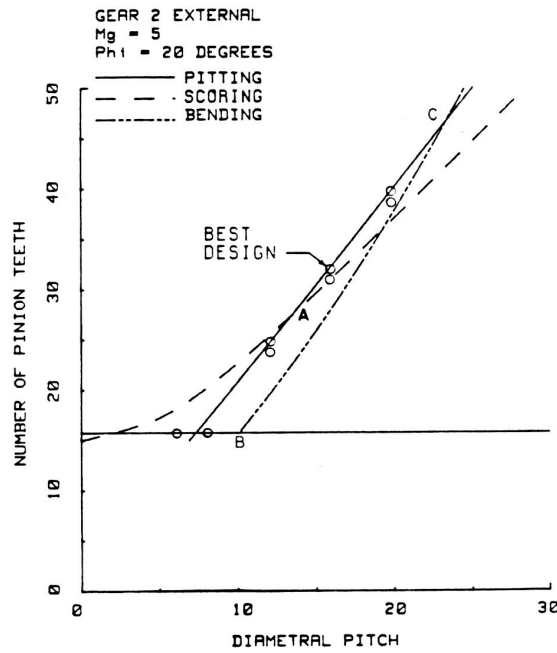


Figure 13. - External gear mesh design space with  $\lambda = 0.25$ ,  $T_p = 113$  N-m (1000 lb-in),  $\sigma_N = 1.38$  GPa (200 ksi),  $\sigma_B = 414$  MPa (60 ksi),  $E = 205$  GPa ( $30 \times 10^3$  ksi),  $v = 0.25$ .

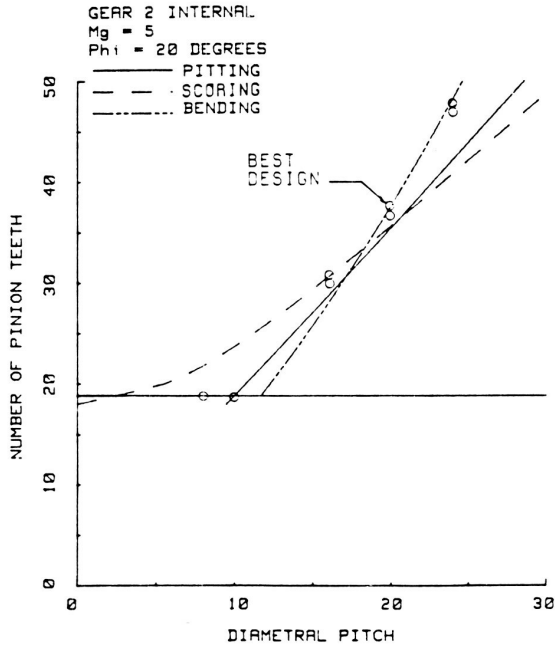


Figure 14. - Internal gear mesh design space with  $\lambda = 0.25$ ,  $T_p = 113$  N-m (1000 lb-in),  $\sigma_N = 1.38$  GPa (200 ksi),  $\sigma_B = 414$  MPa (60 ksi),  $E = 205$  GPa ( $30 \times 10^3$  ksi),  $v = 0.25$ .

To illustrate the effect of gear ratio on the design space, this parameter has been varied for the conditions of figure 12. Figures 13 to 15 show the design space as this ratio changes from 1 to 5 for contact with an external gear and then continuing for contact with an internal gear of increasing conformal contact with ratios of 5 and 2.5.

A continuous change in characteristics occurs as the external gear ratio increases to infinity (contact with a rack) and the internal gear ratio reduces from infinity. Three distinct shifts occur in the design space as the gear ratio increases. First, the involute interference limit increases to a higher number of pinion teeth. Second, point A—the condition of equal surface contact pressure at the gear tip and at the lowest point of single tooth contact—shifts to a higher  $N_1$  and a higher  $P_d$ . Third, the bending fatigue strength limit becomes more critical as the gear ratio increases.

The design tradeoff between pitting fatigue and bending fatigue is shown in the design space curves at the point where these two constraint curves cross (point C in fig. 13). If one were just concerned with bending fatigue failure, a reduction in the number of teeth from point C would produce a better design. Conversely, if one were just concerned with pitting fatigue, an increase in the number of teeth would produce a better design.

Figures 16 to 19 illustrate the effect of a  $25^\circ$  pressure angle on the design space for the same set of gear ratios. Basically, the same conclusions are present as for the  $20^\circ$  pressure angle design spaces. The increase in pressure angle also reduces the minimum number of pinion teeth required to avoid interference, and it reduces the bending load while it increases the bending strength, so the bending fatigue limit becomes less important as the pressure angle is increased. However, the pitting fatigue limit only improves a small amount, so increasing the pressure angle should not significantly improve the surface wear properties of a gearset.

These design spaces indicate that the most compact designs will have a minimal number of teeth. However, this number is not based on involute interference as implied by point B but is based on equal contact pressure at the base of the tooth and in the region of single-tooth contact. Figures 20 and 21 are plots of the numbers of teeth which produce this equality of contact pressure, assuming equal load sharing when two tooth sets are in contact. The upper branch of each curve is for contact

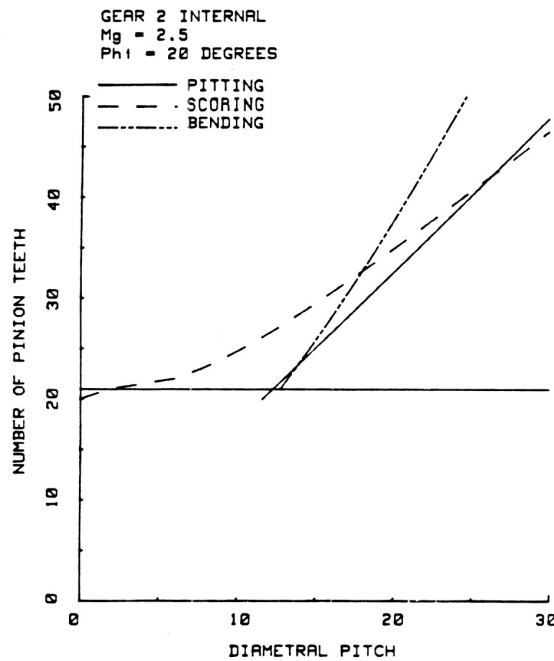


Figure 15. - Internal gear mesh design space with  $\lambda = 0.25$ ,  $T_p = 113$  N-m (1000 lb-in),  $\sigma_N = 1.38$  GPa (200 ksi),  $\sigma_B = 414$  MPa (60 ksi),  $E = 205$  GPa ( $30 \times 10^3$  ksi),  $\nu = 0.25$ .

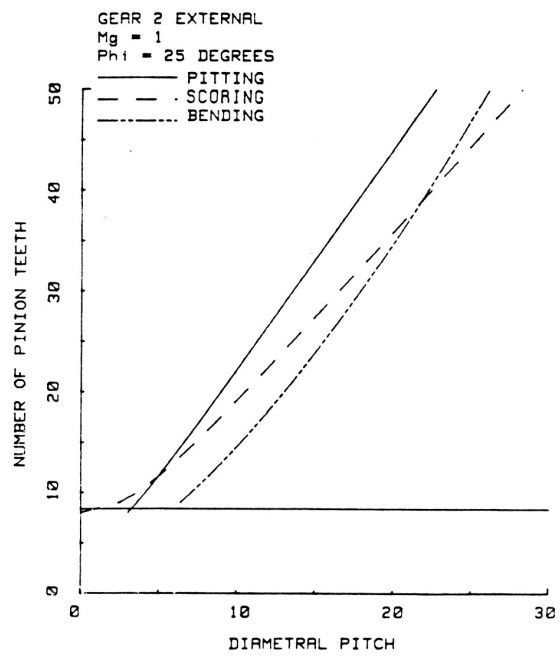


Figure 16. - External gear mesh design space with  $\lambda = 0.25$ ,  $T_p = 113$  N-m (1000 lb-in),  $\sigma_N = 1.38$  GPa (200 ksi),  $\sigma_B = 414$  MPa (60 ksi),  $E = 205$  GPa ( $30 \times 10^3$  ksi),  $\nu = 0.25$ .

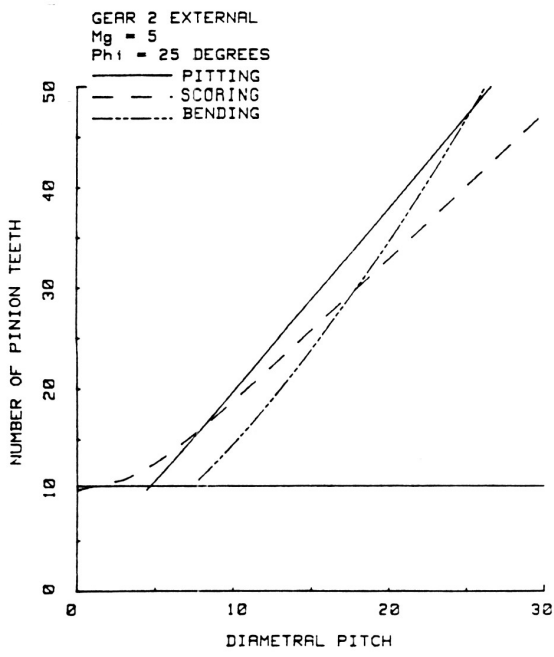


Figure 17. - External gear mesh design space with  $\lambda = 0.25$ ,  $T_p = 113$  N-m (1000 lb-in),  $\sigma_N = 1.38$  GPa (200 ksi),  $\sigma_B = 414$  MPa (60 ksi),  $E = 205$  GPa ( $30 \times 10^3$  ksi),  $\nu = 0.25$ .

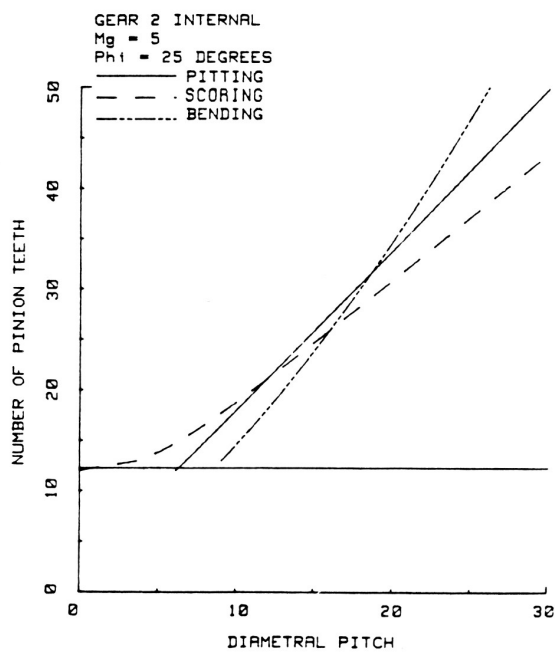


Figure 18. - Internal gear mesh design space with  $\lambda = 0.25$ ,  $T_p = 113$  N-m (1000 lb-in),  $\sigma_N = 1.38$  GPa (200 ksi),  $\sigma_B = 414$  MPa (60 ksi),  $E = 205$  GPa ( $30 \times 10^3$  ksi),  $\nu = 0.25$ .

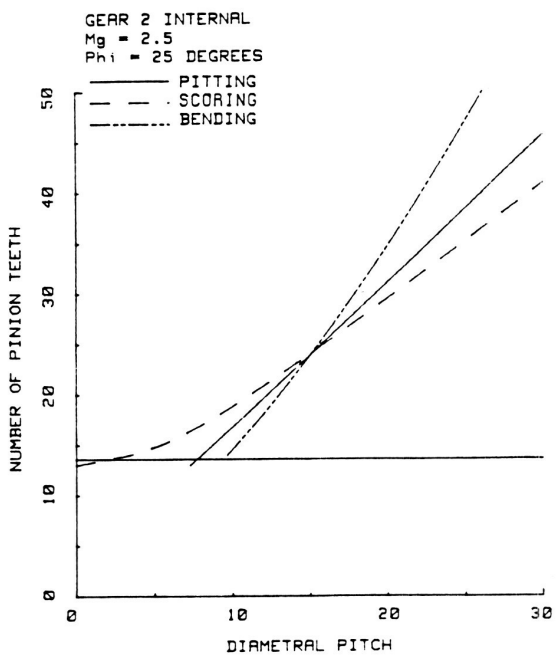


Figure 19. - Internal gear mesh design space with  $\lambda = 0.25$ ,  $T_p = 113$  N-m (1000 lb-in),  $\sigma_N = 1.38$  GPa (200 ksi),  $\sigma_B = 414$  MPa (60 ksi),  $E = 205$  GPa ( $30 \times 10^3$  ksi),  $\nu = 0.25$ .

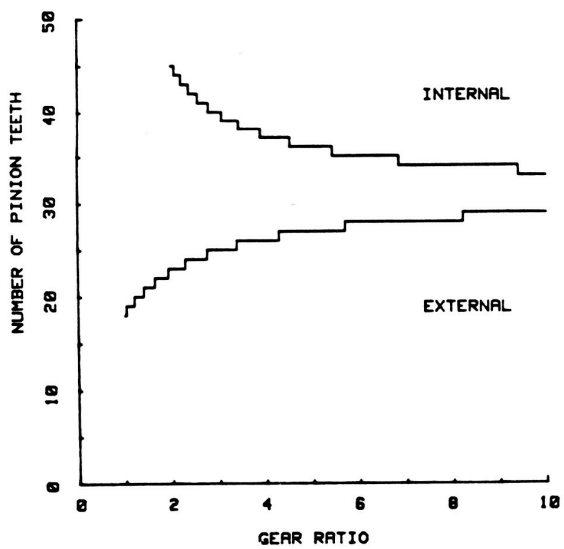


Figure 20. - Optimal number of pinion teeth for 20° pressure angle.

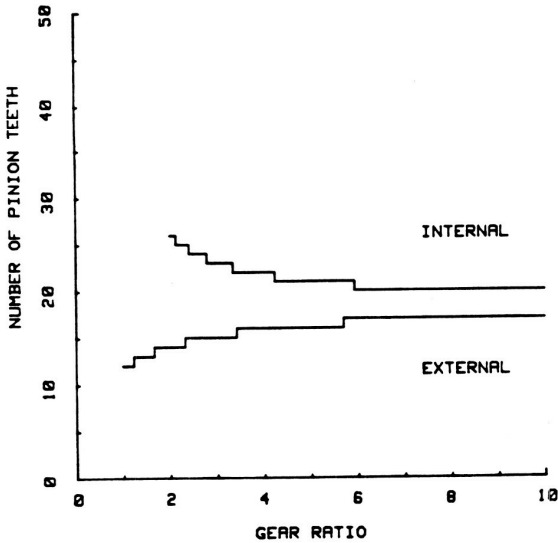


Figure 21. - Optimal number of pinion teeth for 25° pressure angle.

with an internal gear, while the lower branch is for contact with an external gear. Figure 20 is for  $20^\circ$  pressure angle while figure 21 is for  $25^\circ$  pressure angle standard tooth systems. A truly optimal design might use a slightly higher number of teeth in order to obtain a combination of gears with a standard diametral pitch and whole teeth.

## Design Example

To illustrate the use of this method in design, consider a gear ratio of 5 and a pressure angle of  $20^\circ$ . Consider the pinion torque to be 113 N·m (1000 lb·in) and the other design values to be identical to those of figure 13 for convenience. For contact with an external gear, figure 20 indicates that for an optimal design using standard teeth, the pinion should have about 27 teeth. The design space for this particular example is shown in figure 13. One could check the design space of figure 13 to identify point A for which the diametral pitch is about 13.5.

Since this pitch would require nonstandard tooling, the best design will be shifted away from point A. However, it will lie near the pitting constraint line. This pitting constraint line can be closely approximated by a straight line from the origin through point A, with the slope given by

$$k = \frac{N_1}{P_d} \quad (65)$$

In this case

$$k = \frac{27}{13.5} = 2.0$$

The standard pitches near 13.5 can be used to find the numbers of teeth for near optimal designs with equation (65). Pitches of 12, 16, and 20 could be used to obtain minimal numbers of teeth of 24, 32, and 40, respectively. The best design will be in the set of trial designs with pinion teeth numbers near these limits.

Table 2 lists the possible optimum designs determined from equation (65) with diametral pitches of 12, 16, or 20. The best design is that with a  $P_d$  of 16 and 32 pinion teeth. This design has a center distance of 0.152 m (6.0 in.), a maximum contact pressure of 1.35 GPa (196 ksi), and a maximum fillet bending stress of 303 MPa (44 ksi). The design is shown in figure 22. Figure 23 is a plot of the maximum surface compression on the pinion tooth as a function of pinion roll angle.

TABLE 2 EXTERNAL GEAR DESIGNS

$m_g = 5, \phi = 20^\circ$

$P_d$	$N_1$	$N_2$	$f$	$C$	$\sigma_{Nt}$ GPa	$\sigma_N$ GPa	$\sigma_B$ MPa	$\sigma_{BT}$ MPa
-	-	-	m	m				
12	24	120	.0127	.152	1.51	1.39	228	248
12	25	125	.0132	.159	1.37	1.30	207	228
16	31	155	.0123	.148	1.34	1.43	297	331
16	32	160	.0127	.152	1.26	1.35	276	303
20	39	195	.0124	.149	1.21	1.39	338	379
20	40	200	.0127	.152	1.16	1.34	324	359
8	16	80	.0127	.152	6.87	1.49	193	200
6	16	80	.0169	.203	4.45	.97	83	83

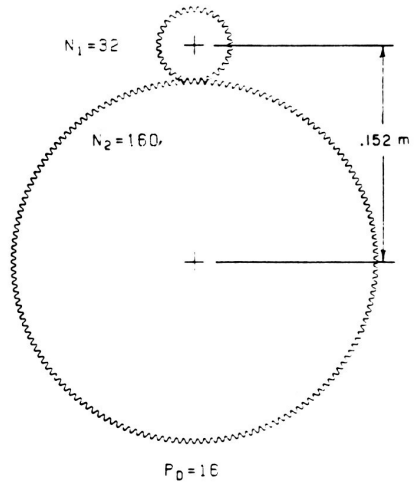


Figure 22. - Optimum design for  $m_g = 5$ ,  $\phi = 20^\circ$ , and  $T_p = 113$  N-m (1000 lb-in) for mesh with external gear.

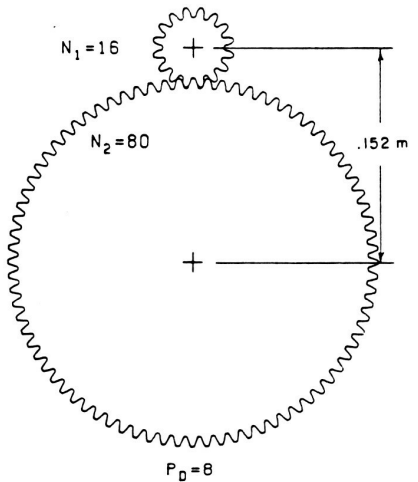


Figure 24. - Minimum tooth number design for  $m_g = 5$ ,  $\phi = 20^\circ$ , and  $T_p = 113$  N-m (1000 lb-in) for mesh with external gear.

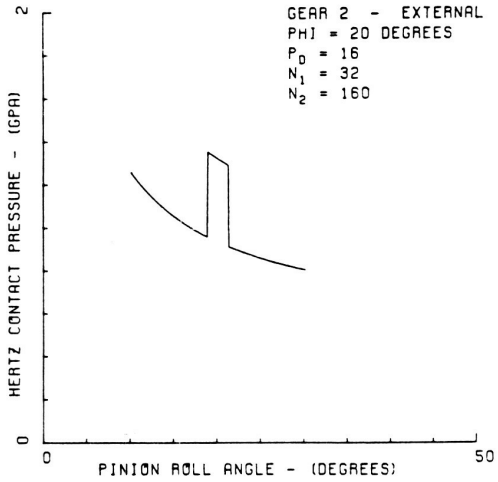


Figure 23. - Optimal external gear design-tooth surface pressure.

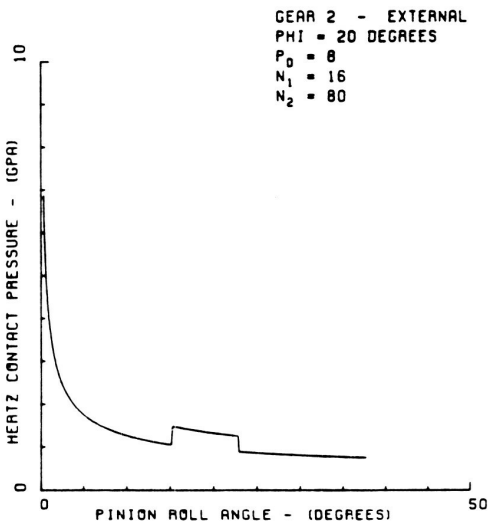


Figure 25. - Minimum tooth number design-tooth surface pressure for mesh with external gear.

It can be noted from table 2 that an equally compact design exists with a diametral pitch of 20 and 40 pinion teeth. This design also has a center distance of 0.152 m (6.0 in.) and does not exceed any of the design stress limits. However, it has 25 percent higher bending stresses with no improvement in compactness, so the lower pitch design is to be preferred.

A popular approach to the design of a gear mesh (ref. 7) suggests that the strongest gear design results when the pinion has the smallest number of teeth possible. This makes the teeth large. Based on the minimum number of teeth required to eliminate interference,  $N_1$  would equal 16. The last two designs in table 2 show this design with a diametral pitches of 8 and 6.

As can be seen in table 2, even decreasing the diametral pitch to 6 to further increase the tooth size does not reduce the scoring contact pressure,  $\sigma_{NT}$ , to the levels present in the optimum design. Figure 24 shows the minimum tooth design with a diametral pitch of 8 and a center distance of 0.152

m (6.0 in.), which is the same as that of the optimal design. This design is stronger than the design of figure 22 in bending fatigue and slightly weaker in pitting fatigue, but is extremely overloaded with contact pressure at the gear tip where scoring may occur. Figure 25 is a plot of the maximum surface pressure on the pinion tooth of this design as a function of pinion roll angle.

A similar study for a gear ratio of 5 and a pressure angle of  $20^\circ$  for contact with an internal gear produces similar results. The major difference lies in the increased levels of bending stress. However, the optimal designs are still in the region of point *A* because of the balance between the strengths given by these proportions.

For this example consider the pinion torque to be 113 N·m (1000 lb·in) and the other design values to be identical to those of the first example with the exception that the gear ratio of 5 is for contact with an internal gear. In this example, both gears turn in the same direction. The design space for this example is shown in figure 14.

Figure 20 indicates that an optimal design using standard teeth should have a pinion with about 36 teeth. In figure 14 point *A* corresponds to a diametral pitch of about 21. Although the bending limit is more critical for this case, if one used this point to obtain a minimum slope relationship between pinion teeth and diametral pitch, equation (65) would yield

$$k = \frac{36}{21} = 1.71$$

Using diametral pitches of 16, 20, and 24, the minimum required number of teeth as given by equation (61) are 27.4, 34.3, and 41.1 respectively. Table 3 lists the possible optimum designs that have these diametral pitches and numbers of pinion teeth greater than these limits. To satisfy the bending fatigue limit, the numbers of teeth in this table are greater than those indicated by equation (65), which is based on the surface pitting pressure. However, the final optimal design is still close to the starting point *A*, so this stands as a good initial design even though the bending fatigue limit controls the design.

The best design is that with a diametral pitch of 20 and 38 pinion teeth. This design has a center distance of 0.0965 m (3.8 in.), a maximum contact pressure of 1.2 GPa (174 000 psi), and a maximum fillet bending stress of 407 MPa (59 000 psi). The design is shown in figure 26. Figure 27 is a plot of the maximum surface compression on the pinion tooth as a function of pinion roll angle.

As in the external contact case, the effect of increasing the diametral pitch in this area of optimal design is to increase the bending stresses.

The last two designs in table 3 show what happens when the design is based on the minimum number of teeth required to prevent involute interference. As before, decreasing the diametral pitch makes the gearset larger but does not change the situation of poor balance between the different modes of failure. Thus, a design that is larger than the optimal design still does not have acceptable levels of surface compression. The design with a diametral pitch of 10 and a center distance of 0.0965

TABLE 3 INTERNAL GEAR DESIGNS

$$m_g = 5, \phi = 20^\circ$$

$P_d$	$N_1$	$N_2$	$f$	$C$	$\sigma_{Nt}$	$\sigma_N$	$\sigma_B$	$\sigma_{BT}$
-	-	-	m	m	GPa	GPa	MPa	MPa
16	30	150	.0119	.095	1.40	1.25	290	352
16	31	155	.0123	.098	1.30	1.19	269	331
20	37	185	.0118	.094	1.23	1.25	352	427
20	38	190	.0121	.097	1.17	1.20	331	407
24	47	235	.0124	.099	1.02	1.13	359	434
24	48	240	.0127	.102	.99	1.10	345	414
10	19	95	.0121	.097	8.27	1.32	207	255
8	19	95	.0151	.121	5.93	0.94	103	131

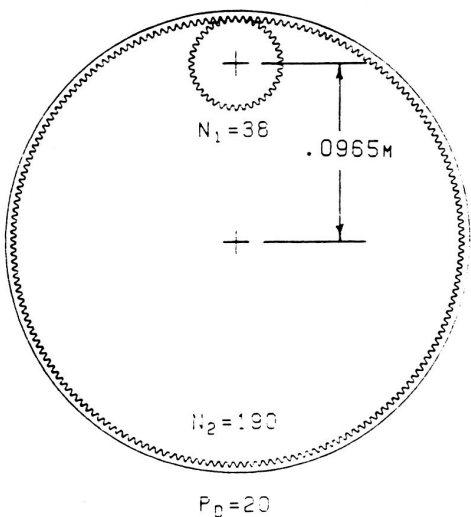


Figure 26. - Optimum design for  $m_g = 5$ ,  $\phi = 20^\circ$ , and  $T_p = 113 \text{ N-m}$  (1000 lb-in) for mesh with internal gear.

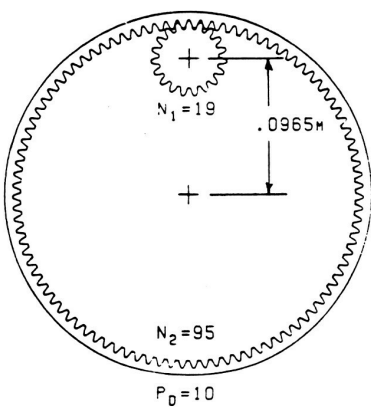


Figure 28. - Minimum tooth number design for  $m_g = 5$ ,  $\phi = 20^\circ$ , and  $T_p = 113 \text{ N-m}$  (1000 lb-in) for mesh with internal gear.

$m$  (3.8 in.) is shown in figure 28. As in the first example, this design is the same size as the optimal design. It also is stronger in bending than the optimal design but is greatly overloaded with contact pressure at the gear tip where scoring may occur. Figure 29 is a plot of the maximum surface pressure on the pinion tooth of this design as a function of pinion roll angle.

## Design Procedure

The design space developed in this paper can be used to obtain optimal designs for gear meshes using standard spur gears. A procedure using this design space was followed in the two design examples of the previous section. Required input to the procedure is the gear ratio, the pinion torque

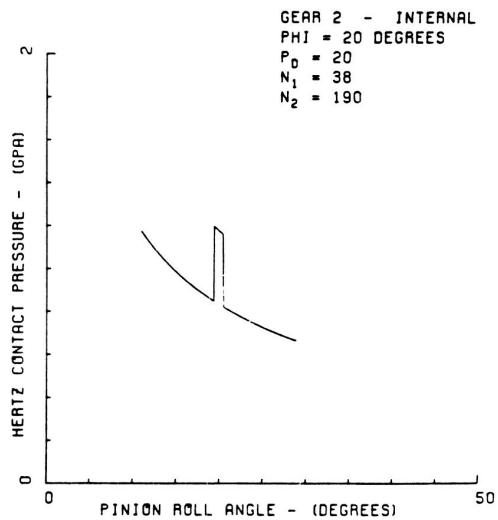


Figure 27. - Optimal internal gear design-tooth surface pressure.

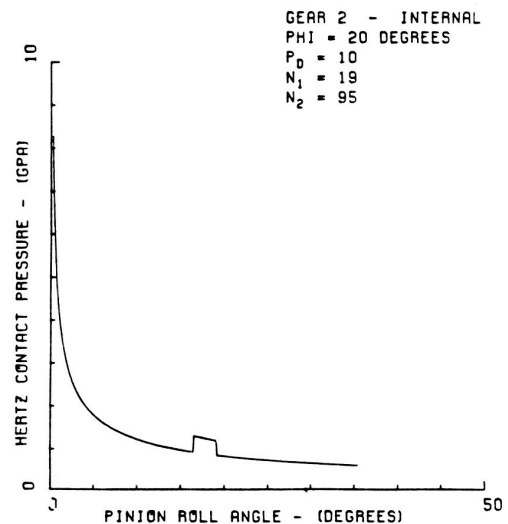


Figure 29. - Minimum tooth number design-tooth surface pressure for mesh with internal gear.

the pitch-line pressure angle, the maximum allowable length to diameter ratio for the pinion pitch cylinder, and the material properties of the gears. Equation (10) or (17) can then be used to determine the kinematic interference limit for the mesh, and equations (59), (61), and (62) can be used to determine the strength constraints on the design space. By plotting these curves on a graph of pinion tooth number versus diametral pitch, the region of acceptable designs can be established as that region of high pinion tooth numbers and low diametral pitches bounded by these curves. The most compact designs lie on the line of least slope inside this region. For designs in which surface pressure dominates, the graphs of figures 20 and 21 show the optimal number of pinion teeth as a function of the gear ratio and pressure angle. By using the number of pinion teeth indicated by these graphs and a straight line through the origin, a set of standard pitches and corresponding minimum numbers of pinion teeth can be found near this optimal position. A small set of standard pitch, practical designs can now be obtained by considering designs with these pitches and valid numbers of pinion teeth greater than the corresponding minimum numbers. By analyzing these designs and comparing their properties, a practical optimum design can be selected.

## Summary and Conclusions

A design procedure for sizing standard involute spur gearsets is presented in this paper. The procedure is applied to find the optimal design for two examples—an external gear mesh with a ratio of 5:1 and an internal gear mesh with a ratio of 5:1. In the procedure, the gear mesh is designed to minimize the center distance for a given gear ratio, pressure angle, pinion torque, and allowable tooth strengths.

From the methodology presented, a design space may be formulated for either external gear contact or for internal gear contact. The design space includes kinematics considerations of involute interference, tip fouling, and contact ratio. Also included are design constraints based on bending fatigue in the pinion fillet and Hertzian contact pressure in the full load region and at the gear tip where scoring is possible. This design space is two-dimensional, giving the gear mesh center distance as a function of diametral pitch and the number of pinion teeth. The following results were obtained:

1. The constraint equations were identified for kinematic interference (eqs. (10) and (17)), fillet bending fatigue (eq. (59)), pitting fatigue (eq. (61)), and scoring pressure (eq. (62)), which define the optimal design space for a given gear design.
2. The locus of equal size optimum designs was identified as the straight line through the origin which has the least slope in the design region.
3. For designs in which bending fatigue is not dominant, the optimal design condition was identified as the point in the design space where the tooth tip contact pressure equals the maximum full load contact pressure.
4. Design charts for selecting the optimal number of pinion teeth for a given gear ratio and pressure angle were presented for these cases.

## References

1. Cockerham, G.; and Waite, D.: Computer-Aided Design of Spur on Helical Gear Train. *Computer-Aided Design*, vol. 8, no. 2, April 1976, pp. 84-88.
2. Tucker, A. I.: The Gear Design Process. ASME Paper 80-C2/DET-13.
3. Estrin, M.: Optimization of Tooth Proportions for a Gear Mesh. ASME Paper 80-C2/DET-101.
4. Gay, D. E.: How to Design to Minimize Wear in Gears. *Machine Design*, vol. 42, Nov. 1970, pp. 92-97.
5. Design Procedure for Aircraft Engine and Power Take-Off Spur and Helical Gears. AGMA Standard No. 411.02, Sep. 1966.
6. Dudley, D. W.: *Gear Handbook*. McGraw Hill Book Co., Inc., 1962.
7. Shigley, J. E.: *Mechanical Engineering Design*. McGraw Hill Book Co., Inc., 3rd ed., 1977.
8. Lee, T. W.: Weight Minimization of a Speed Reducer, ASME Paper 77-DET-163.
9. Osman, M. O. M.; Sankar, S.; and Dukkipati, R. V.: Design Synthesis of a Multi-Speed Machine Tool Gear Transmission Using Multiparameter Optimization. *J. Mech. Des.*, vol. 100, April 1978, pp. 303-310.
10. Kamenatskaya, M. P.: Computer-Aided Design of Optimal Speed Gearbox Transmission Layouts. *Mach. & Tool.*, vol. 46, no. 9, 1975, pp. 11-15.

11. Buckingham, E.: *Analytical Mechanics of Gears*. McGraw Hill Book Co., Inc., 1949.
12. Anderson, S. A. E.: On the Design of Internal Involute Spur Gears. *Transactions of Machine Elements Division*, Lund Technical University, Lund, Sweden, 1973.
13. Strength of Spur Gear Teeth. AGMA Standard 220.02, August 1966.
14. Gitchel, K. R.: Computed Strength and Durability Geometry Factors for External Spur and Helical Gears with Tooling Check. ASME Paper 72-PTG-18.
15. Mitchiner, R. G.; and Mabie, H. W.: The Determination of the Lewis Form Factor and the AGMA Geometry Factor J for External Spur Gear Teeth. *J. Mech. Des.* V104, Jan. 1982, pp. 148-158.16. Surface Durability (Pitting) of Spur Gear Teeth. AGMA Standard 210.02, Jan. 1965.
17. Coy, J. J.; Townsend, D. P.; and Zaretsky, E. V.: Dynamic Capacity and Surface Fatigue Life for Spur and Helical Gears. *J. Lubr. Technol.*, vol. 98, no. 2, April 1976, pp. 267-276.
18. Bowen, C. W.: The Practical Significance of Designing to Gear Pitting Fatigue Life Criteria. *J. Mech. Des.*, vol. 100, no. 1, Jan. 1978, pp. 46-53.
19. Gear Scoring Design Guide for Aerospace Spur and Helical Power Gears. AGMA Information Sheet, 217.01, Oct. 1965.
20. Rozeana, L.; and Godet, M.: Model for Gear Scoring. ASME Paper 77-DET-60.
21. Walker, H.: Gear Tooth Deflection and Profile Modification. *The Engineer*, Oct. 14, 1938, pp. 409-412; Oct. 21, 1938, pp. 434-436; Aug. 16, 1940, pp. 102-104.
22. Coleman, W.: Gear Design Considerations. *Interdisciplinary Approach to the Lubrication of Concentrated Contacts*. NASA SP-237, 1969.